

5.2. Palmer Station (7/17/02 – 3/17/03)

The 2002-2003 season at Palmer Station is defined as the time between the system service in 2002, which took place between 7/9/02 and 7/17/02, and the site visit in 2003, performed between 3/17/03 and 3/24/03. Season opening absolute calibrations were performed between 7/15/02 and 7/16/02; season closing calibrations were carried out on 3/17/03. Volume 12 solar data comprise the period 7/17/02 – 3/17/03. In general, the system performed as expected. Only 8 out of 15615 scans were lost due to technical problems. No PSP data is available for the period 1/15/03 – 1/24/03 due to a defective instrument cable.

This is the first season when a GUV-511 moderate-bandwidth filter radiometer (see Section 2) was installed at Palmer Station next to the collector of the SUV-100. Data of the instrument is available for interested researchers. See Section 5.2.5 for further details.

5.2.1. Irradiance Calibration

The site irradiance standards for 2002-2003 were the lamps 200W007, M-765, and M-700. Lamp M-764 was used as the traveling standard at the beginning and end of the season. It was calibrated by Optronic Laboratories in March 2001.

Lamp 200W007 has an irradiance calibration from Optronic Laboratories from November 1996. Lamp M-765 has an Optronic Laboratories calibration from 1992 and has been in use at Palmer Station since 1992. The lamp was recalibrated with the previous traveling standard M-874 using data from the Volume 9 opening calibrations. Lamp M-700 was calibrated in a similar fashion as lamp M-765; the irradiance calibration was transferred from the traveling standard M-874 using absolute scans of both lamps from days 5/11/99 and 5/12/99. The calibrations of all three site standards were the same as in Volume 10 and Volume 11. Figure 5.2.1 shows the Volume 12 season opening calibrations. All site standards agree on the $\pm 1\%$ level. There is a bias of 0.5-1.5% compared to the calibration of the traveling standard M-764. Figure 5.2.2 shows the Volume 12 season closing calibrations performed on 3/17/03. All lamps agree with M-764 to within $\pm 1\%$. The result is very consistent to the season opening calibrations.

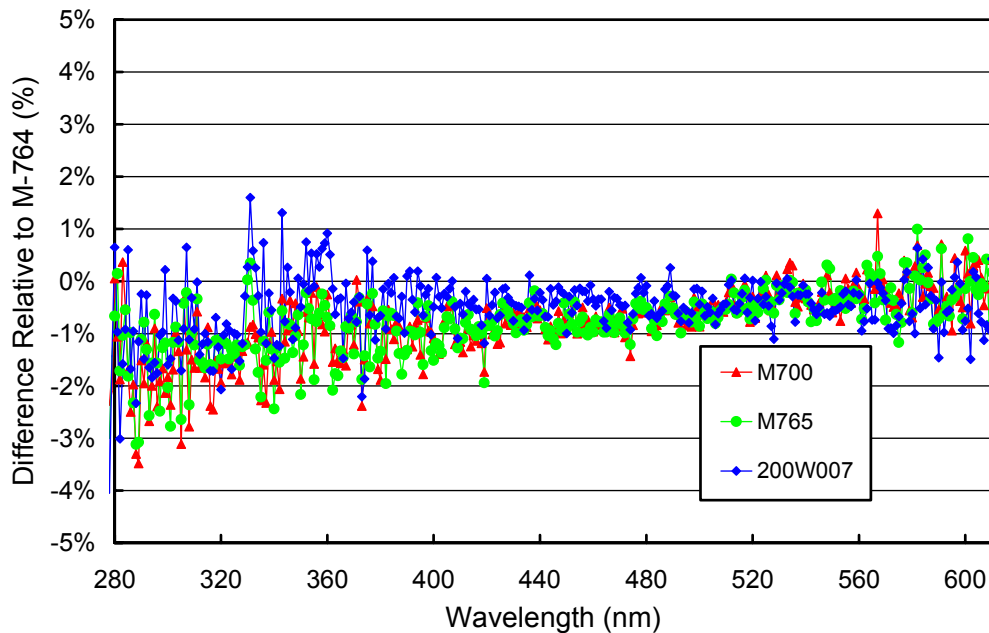


Figure 5.2.1. Comparison of Palmer lamps 200W007, M-700, and M-765 with the BSI traveling standard M-764 at the beginning of the season (7/15/02 and 7/16/02).

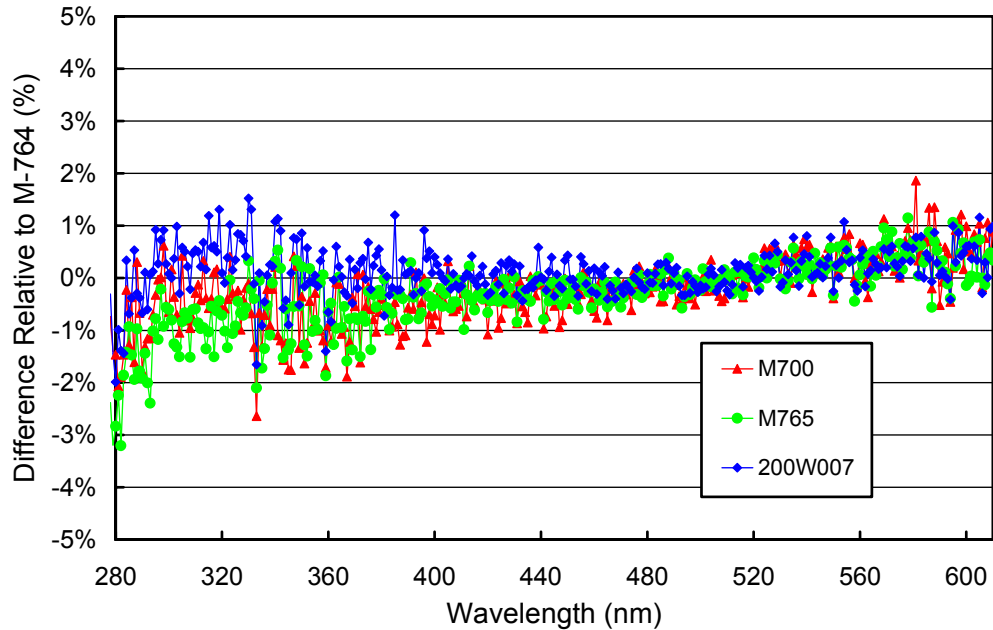


Figure 5.2.2. Comparison of Palmer lamps 200W007, M-700, and M-765 with the BSI traveling standard M-764 at the end of the season (3/17/03).

5.2.2. Instrument Stability

The stability of the spectroradiometer over time is primarily monitored with bi-weekly calibrations utilizing the site irradiance standards and daily response scans of the internal irradiance reference. The stability of the internal lamp itself is monitored with the TSI sensor, which is independent from possible monochromator and PMT drifts. By logging the PMT currents at several wavelengths during response scans, changes in the instrument responsivity can be detected.

Figure 5.2.3 shows the changes in TSI readings and PMT currents at 300 and 400 nm, derived from the daily response scans of the Palmer 2002/03 season. The TSI measurements indicate that the internal lamp was stable to within $\pm 1.5\%$; PMT currents were stable to within $\pm 2\%$, and track the TSI measurements well.

Although analysis of the response scans suggested good stability of the system, calibrations with 200-Watt lamps indicated that the radiometric accuracy of the instrument can be improved by breaking the season into five periods with different absolute calibrations applied in each period. Figure 5.2.4 shows the ratio of these spectra, referenced to the first spectrum. Period 1 (i.e. the period of the reference spectrum) encompasses only the first three days after the site visit (7/17/02 – 7/19/02). Figure 5.2.4 indicates that there is a 2-4% change in responsivity between Period 1 and 2, suggesting that the system had not fully stabilized when solar scanning commenced. Calibrations of Period 3 (10/8/02 - 11/29/02) and Period 5 (1/8/03 - 3/19/03) are almost identical, however, the calibration of Period 4 is higher by about 2%.

The standard deviation of the individual spectra contributing to the average spectrum for each calibration period were calculated. Figure 5.2.5 shows the ratio of the standard deviation and average spectra. The ratios are useful for estimating the variability of the calibrations and the consistency of the different site standards in each period. Figure 5.2.5 shows that the standard deviation is usually less than 1.2% of the average for all periods in the UV-A and visible, and increases slightly towards shorter wavelengths. The spike at 332 nm in the plot of Period 3 is caused by an anomalous value in one calibration spectrum and the fact that the calibration spectrum for Period 3 is only based on four absolute scans.

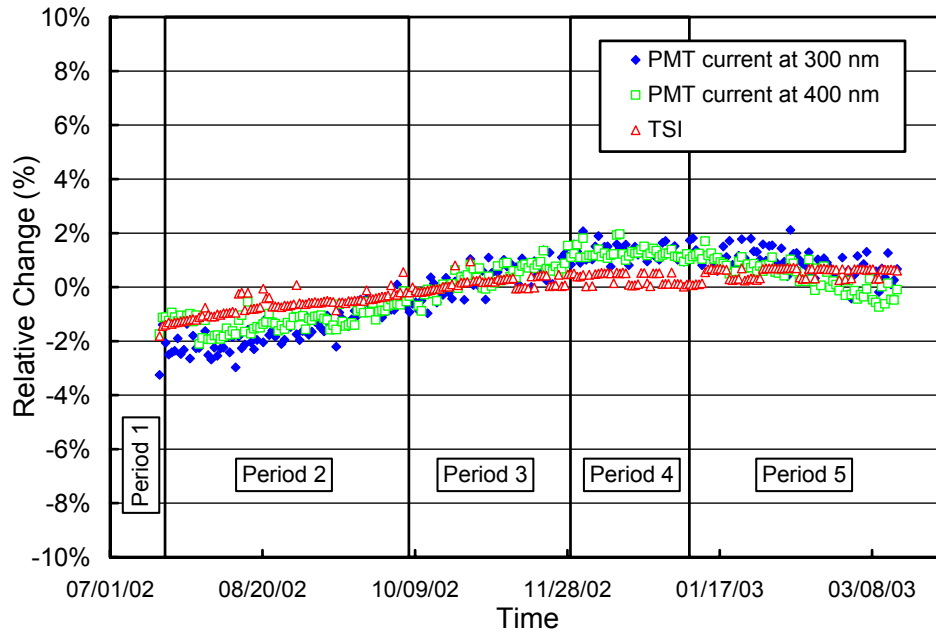


Figure 5.2.3. Time-series of PMT current at 300 and 400 nm, and TSI signal during measurements of the response lamp during the Palmer 2002/03 season. The data is normalized to the average of all periods.

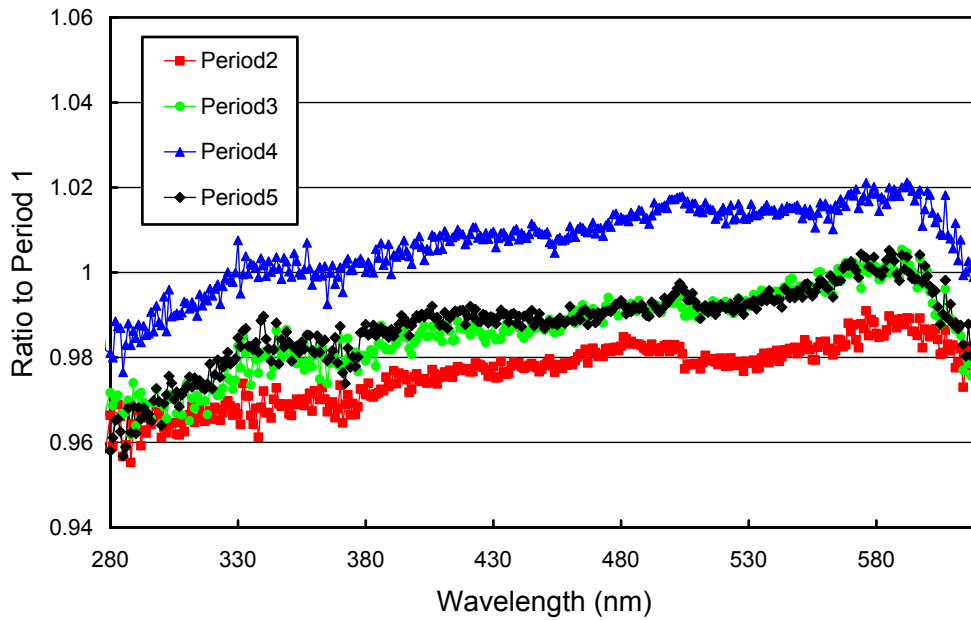


Figure 5.2.4. Ratios of irradiances assigned to the internal reference lamp compared to Period 1.

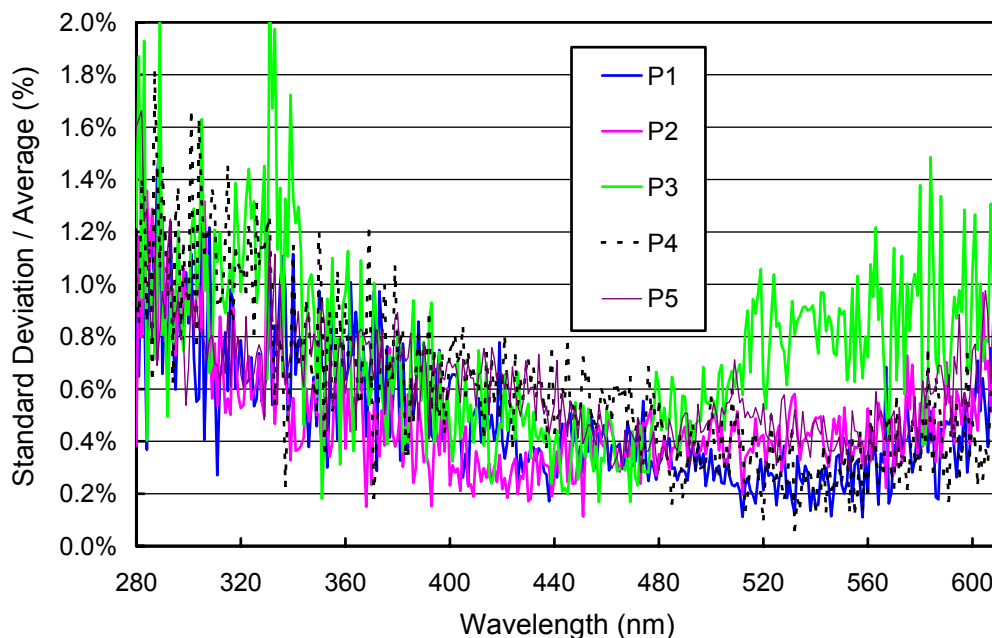


Figure 5.2.5. Ratio of standard deviation and average calculated from the absolute calibration scans.

5.2.3. Wavelength Calibration

Wavelength stability of the system was monitored with the internal mercury lamp. Information from the daily wavelength scans was used to homogenize the data set by correcting day-to-day fluctuations in the wavelength offset. After this step, there may still be a deviation from the correct wavelength scale, but this bias should ideally be the same for all days. Figure 5.2.6 shows the differences in the wavelength offset of the 296.73 nm mercury line between two consecutive wavelength scans. In total, 244 scans were evaluated. For 99% of the days, the change in offset was smaller than ± 0.25 nm; the largest change in offset was 0.027 nm. The excellent wavelength stability can partly be attributed to the new peak finding algorithm, which was first implemented for Palmer Volume 11 data (see Volume 11 Operations Report).

After the data was corrected for day-to-day wavelength fluctuations, the wavelength-dependent bias between this homogenized data set and the correct wavelength scale was determined with the Fraunhofer-correlation method, as described in Section 4. Figure 5.2.7 shows the correction function. After the data was wavelength corrected using this function, the wavelength accuracy was tested again with the Fraunhofer method. The results are shown in Figure 5.2.8 for four UV wavelengths. The residual shifts are generally smaller than ± 0.05 nm. The variation is slightly higher during the first month of the season because of the small solar irradiance levels that prevail during July and August, which affect the correlation algorithm.

Although data from the external mercury scans do not have a direct influence on the data products, they are part of our instrument characterization routine. Figure 5.2.9 illustrates the difference between internal and external mercury scans collected during both site visits. The wavelength scale of the figure is the same as applied during solar measurements. External scans have a bandwidth of about 0.94 nm FWHM; the bandwidth of the internal scan is only 0.75 nm. Internal scans of both periods are shifted by about 0.1 nm to shorter wavelength with respect to their external counterparts. Since external scans have the same light path as solar measurements, they more realistically represent the monochromator bandpass relevant for solar scans.

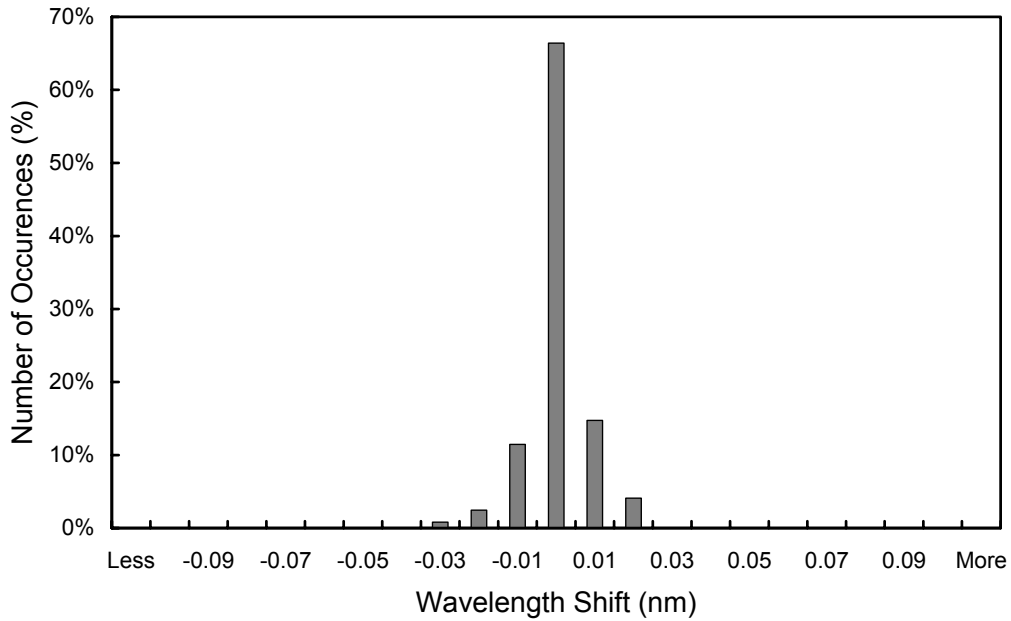


Figure 5.2.6. Differences in the measured position of the 296.73 nm mercury line between consecutive wavelength scans. The x-labels give the center wavelength shift for each column. Thus the 0-nm histogram column covers the range -0.005 to +0.005 nm. “Less” means shifts smaller than -0.105 nm; “more” means shifts larger than 0.105 nm. The excellent wavelength stability can partly be attributed to the new Gaussian peak finding algorithm, which was first implemented for Palmer Volume 11 data.

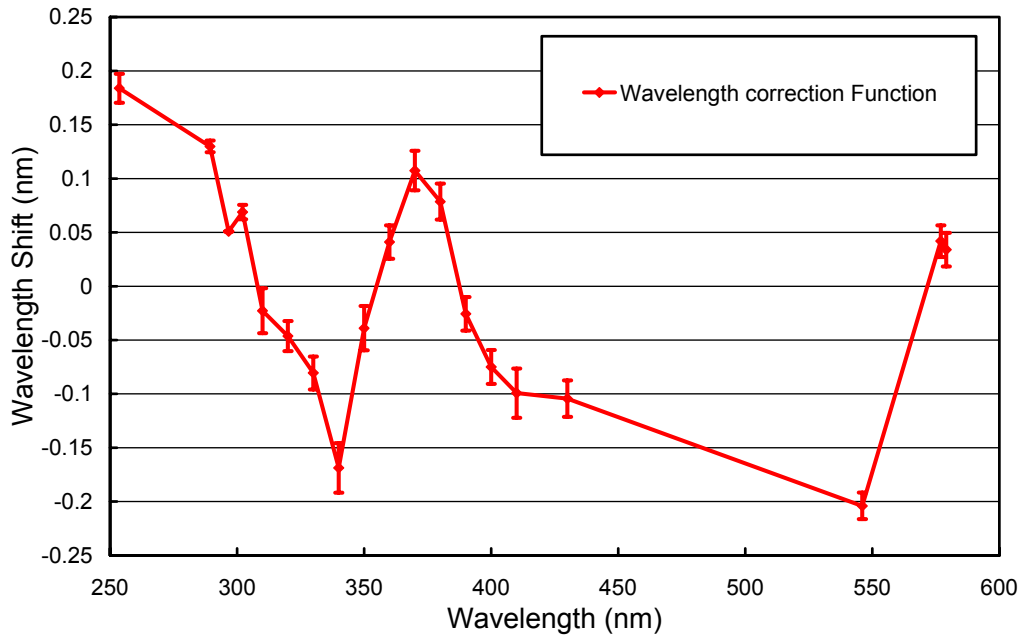


Figure 5.2.7. Monochromator mapping function for the Palmer 2002/03 season.

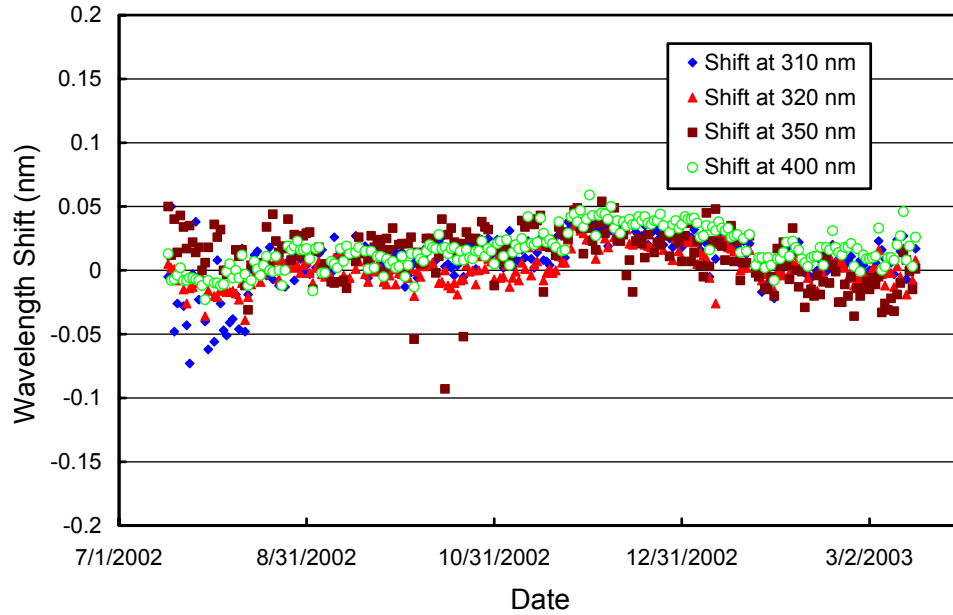


Figure 5.2.8. Wavelength accuracy check of the final data at four wavelengths by means of Fraunhofer correlation. The noontime measurement has been evaluated for each day of the season.

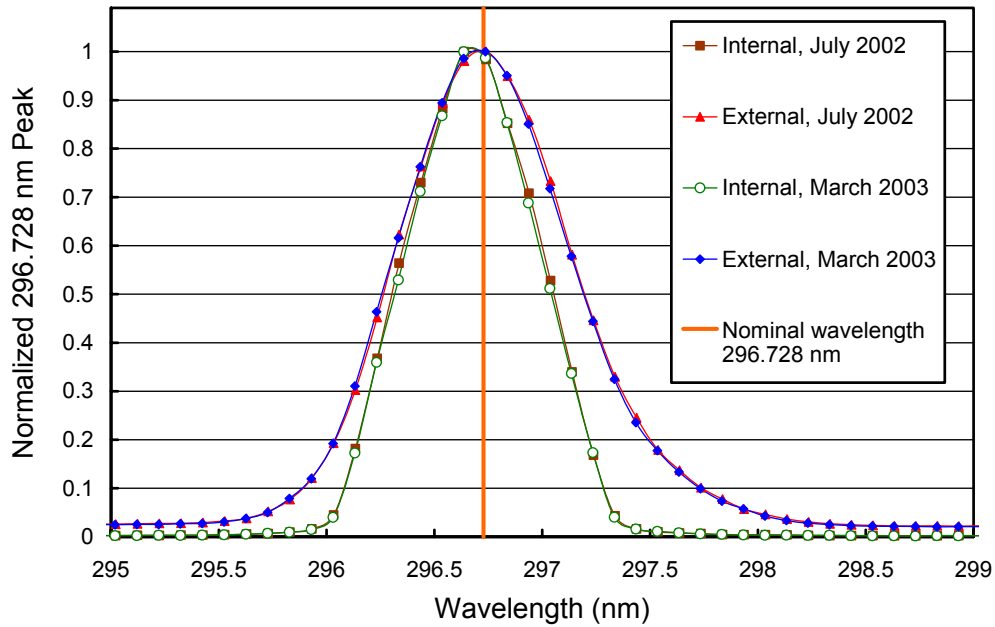


Figure 5.2.9. The 296.73 mercury line as registered by the PMT from external and internal sources. The wavelength scale is the same as applied for solar measurements.

5.2.4. Missing Data

A total of 15615 scans are part of the published Palmer Volume 12 data set. Eight scans scheduled on 10/8/02 are missing because of communication problems between computer and the system's ADC. These are the only scans lost due to technical problems. About 2% of solar scans were superseded by absolute, wavelength, and response scans. Since Palmer Station has almost 24 hours of sunlight per day in December, a loss of data scans cannot be avoided. No PSP data is available for the period 1/15/03 – 1/24/03 because of a defective cable.

5.2.5. GUV Data

During 2001, we started deploying Biospherical Instruments GUV-511 moderate-bandwidth filter radiometer at network sites in close proximity to the collector of the SUV-100. The GUV-511 instrument provides measurements in four approximately 10 nm wide UV bands centered at 305, 320, 340, and 380 nm, as well as photosynthetically active radiation (PAR). From data recorded at these wavelength, total column ozone, spectral integrals, and dose rates for a large number of action spectra is calculated and made available in near real-time via the website <http://www.biospherical.com/nsf/login/update.asp>. Details about calibration and calculation of data products are at http://www.biospherical.com/nsf/presentations/SPIE_paper_5156-23_Bernhard.pdf. In addition to providing data via the Internet, the radiometer is also used to quality control SUV-100 measurements.

Figure 5.2.10. shows a comparison of GUV-511 and SUV-100 erythemal irradiance based on final Volume 12 data. For SZA smaller than 80°, 98.6% of the data agree to within $\pm 10\%$ with each other. The agreement for some data products (e.g. DNA damaging variation) may be worse than that for erythema due to principal limitations in calculating dose-rates from the four GUV-511 channels when the Sun is low and when the data product in question is heavily weighted toward wavelengths below 310 nm. We therefore advise data users to use SUV-100 rather than GUV-511 data when possible, in particular for low-Sun conditions.

Note that a new data set of SUV-100 data, named "Version 2" is currently in preparation (see <http://www.biospherical.com/nsf/Version2/Version2.asp>). Version 2 data are corrected for the cosine error of the SUV-100 spectroradiometer. Version 2 erythemal data are approximately 6% higher than the Version 0 data that are discussed in this report. GUV measurements were calibrated both against cosine error corrected and uncorrected SUV-100 data, and both data sets were published. Preliminary GUV data made available via the website <http://www.biospherical.com/nsf/login/update.asp> are based on the calibration with the cosine corrected SUV-100 data set, and are therefore approximately 6% higher than data plotted in Figure 5.2.10.

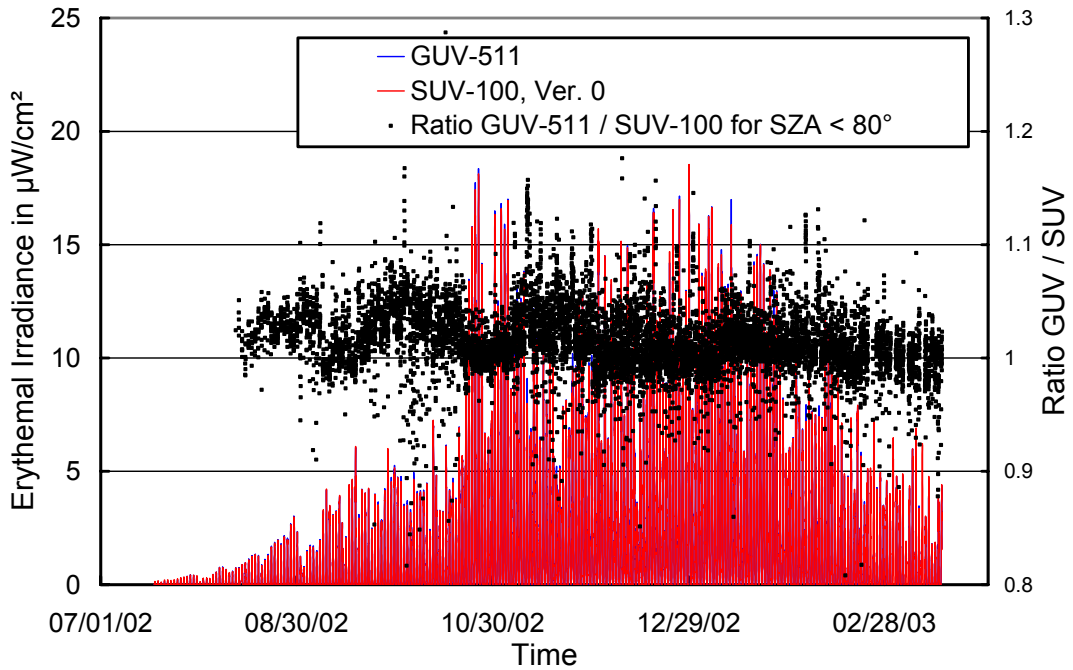


Figure 5.2.10. Comparison of erythemal irradiance measured by the SUV-100 spectroradiometer and the GUV-511 radiometer. All data is based on “Version 0” (cosine-error uncorrected) data.

Figure 5.2.11 shows a comparison of total ozone measurements from the GUV-511 and NASA/TOMS Earth Probe satellite (Version 7). GUV-511 ozone values were calculated as described in http://www.biospherical.com/nsf/presentations/SPIE_paper_5156-23_Bernhard.pdf.

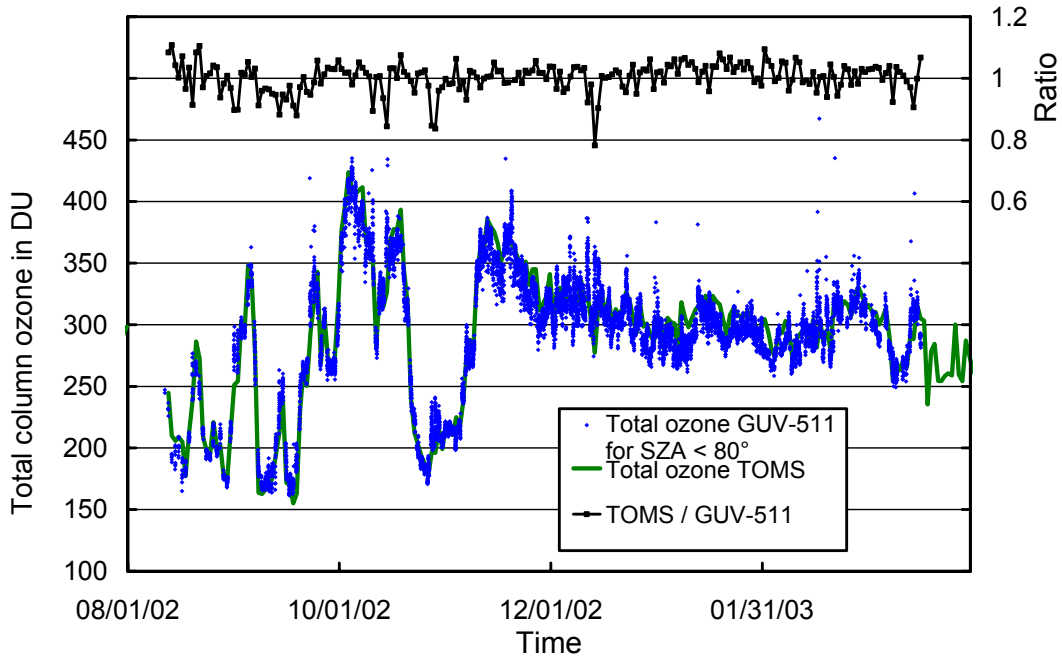


Figure 5.2.11. Comparison of total column ozone measurements from GUV-511 and NASA/TOMS Earth Probe satellite. GUV-511 measurements are plotted in 15 minute intervals. For calculating the ratio of both data sets only GUV-511 measurements coincident with the TOMS overpass were evaluated.